energies

MDPI

Article

Analysis of the All-Year Operation of the Solar Chimney in Polish Climatic Conditions

Sylwia Berdowska

Department of Power Engineering, Częstochowa University of Technology, Al. Armii Krajowej 17, 42-200 Częstochowa, Poland; sylwia.berdowska@pcz.pl

Abstract: This work presents an analysis of the all-year operation of the solar chimney. The analyzed system consists of a rectangular solar collector located on the southern side of the solar chimney. The surface of the solar collector is 30 m^2, while the chimney is 50 m in height. Hourly changes in solar radiation were taken into account in the calculations. The simulation was made for the climatic conditions in Katowice, Poland. This study takes into account the most important parameters of the power plant, such as air temperature, air velocity and power of the installation throughout the year of the power plant's operation. The cumulative amount of electricity that is generated in each month of the year is shown. The analyzed solar power plant produces the largest amount of electricity in the second quarter of the year and the lowest in the fourth quarter, with the maximum amount of energy produced in May and the minimum in December.

Keywords: solar energy; solar chimney power plant; solar collector

Citation: Berdowska, S. Analysis of the All-Year Operation of the Solar Chimney in Polish Climatic Conditions. *Energies* **2022**, *15*, 4738. https://doi.org/10.3390/en15134738

Academic Editor: Surender Reddy Salkuti

Received: 26 May 2022
Accepted: 27 June 2022
Published: 28 June 2022

1. Introduction

With the continued development of civilization, today there is an even greater demand for electricity. As fossil energy sources reach depletion, and due to their negative impact on the natural environment, alternative solutions are constantly being sought as renewable energy. Currently, technologies using solar energy are very popular, including solar collectors and photovoltaic cells.

A solar chimney is a combination of two technologies: an air solar collector and a chimney in which a wind turbine is situated. The ambient air flowing into the installation is heated in the solar collector, which changes its density and, consequently, induces its movement through chimney draft. After passing through the collector, the air is directed to the wind turbine system. The first time a solar chimney was installed was in 1982 in Spain. The system consisted of a chimney, 10 m in diameter and 195 m in height, and a 46,000 m^2 collector with an electric power of 50 kW [1].

Solar chimney installation tests are conducted all over the world in countries with high insolation, for example in India, China, Algeria and Tunisia [2–5]. Scientists from Tunisia analyzed the influence of the shape of the chimney on the behavior of air velocity. The following shapes of chimneys were investigated: a standard chimney, a convergent chimney, a divergent chimney, and an opposing chimney. The maximum air speed was reached in a divergent chimney. Various types of chimneys such as a divergent chimney as well as cylindrical chimneys with a divergent inlet and a divergent outlet were also studied by Hu et al. [6].

Attig-Bahar et al. analyzed the influence of heat accumulation in the ground on which the chimney collector was placed on system efficiency specifically for the climate in Tunisia [7]. Substrates such as soil, gravel, and sand were tested. The relationship between the released and stored thermal energy in the substrate is closely related to the season of the year. The substrate absorbs more heat during the day than is released during the night in spring and summer, while more heat is released during the night in the winter months

than is absorbed during the day. Energy production with a heat storage system produces approximately 35% more energy compared to a chimney installation without heat storage.

Iranian researchers analyzed the solar chimney for 12 selected regions. A solar chimney can meet the electricity demand of towns that do not have access to the electricity network, while its collector is used as an agricultural greenhouse [8]. Bernardes et al. analyzed the influence of various environmental conditions and installation dimensions on the obtained output power [9]. Pretorius et al. investigated the influence of various parameters on the efficiency of the solar chimney, e.g., different types of substrates on which the collector was placed, and the features of the glass used for the collector's roof [10]. The influence of the working fluid on chimney efficiency was also analyzed. The study showed that air is a better working fluid than water [11].

Studies are being carried out on the system of the solar chimney, which is also used to desalinate water. Such a system can generate electricity and desalinate sea water [12–15]. In such a solution, water tanks are placed under the solar collector. Solar chimney systems, which can also be used for food drying, were also analyzed [16]. Currently, systems integrated with a solar chimney are also being researched, e.g., a combination of a solar chimney with photovoltaic panels [17–21].

In the literature, there are cases of small-scale solar chimney research. Parameters such as air temperature, absorber temperature, air velocity and electric power generated were tested in a small solar chimney 6 m in height. The average power of the installation was 0.82 W [22]. Another example may be the analysis of a small installation with a chimney 3 m in height and a 16.4 m^2 collector, where parameters such as electric power, air speed and efficiency were tested. The electric power of the tested installation was from 3 to 20 W, while the efficiency was 0.11% [23]. A small solar chimney located on the roof of the building was also analyzed in the study by Sreejaya et al. [24]. In the Silva and Maia study optimization of the dimensions of the collector diameter, the height of the collector, the height of the chimney and the diameter of the chimney of a small solar chimney were chosen to obtain maximum exergy efficiency [25].

The aim of this article is to analyze the potential of electricity production with the use of a solar chimney in Polish climatic conditions. Calculations were made for a city in Silesia, a region in the south of Poland. For the analysis, a small installation was selected with a chimney 50 m in height and a 30 m^2 rectangular collector located on one side of the chimney. The work for each hour of the year presents the average temperature that is achieved in the collector, the temperature increase in the collector, air velocity in the solar chimney, and the amount of electricity that can potentially be generated by the solar chimney system.

2. Materials and Methods

2.1. Climatic Conditions in the Silesia

Silesia is a region located in the south of Poland. It is the most industrialized region in Poland. It is also the region with the highest population density, which amounts to 364 people/km^2, with the average population density for the whole country amounting to 122 people/km^2 [26], and therefore there is a great demand for electricity in this area. In the south of Poland, during the winter season, there is more solar radiation energy than in other parts of the country, which is influenced by the length of the day and the angle of the sun's rays. In Silesia there is approximately 1400 h of direct solar radiation during the year [27]. The intensity of solar radiation falling on a given surface depends on factors such as cloud cover, transparency of the atmosphere, humidity, and type of air. In the south of Poland, cloud cover is greatest from November to January, and lowest at the turn of summer and autumn.

2.2. Solar Chimney

In this article, calculations were made for the installation of the solar chimney, which consists of a rectangular solar collector 30 m in length and 1 m in width situated on the

southern side of the chimney and a chimney 50 m in height and 1 m in diameter. A wind turbine is placed in the chimney. The air is heated in the solar collector and then directed to the wind turbine system. Figure 1 shows a schema of a solar chimney.

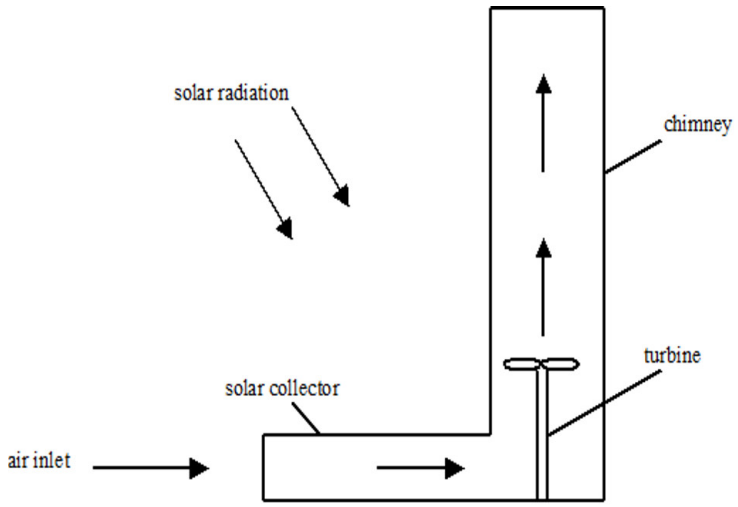

Figure 1. Solar chimney.

2.3. Mathematical Model

2.3.1. Transmission of Solar Radiation through the Collector Glass

The mean transmission-absorption coefficient $(\tau\alpha)$ was determined from the formula [28]:

$$(\tau\alpha) = \frac{G_b R_b (\tau\alpha)_{\theta_\beta} + (G_d R_d + (G_b + G_d)\rho_o R_o)(\tau\alpha)_{60^\circ}}{G_b R_b + G_d R_d + (G_b + G_d)\rho_o R_o} \quad (1)$$

where

G_b—direct radiation flux density on the horizontal plane;
G_d—diffusion radiation flux density on the horizontal plane;
ρ_o—ground reflectance coefficient;
$(\tau\alpha)_{60^\circ}$—transmission-absorption coefficient for the diffusion component, which, assuming isotropy of solar radiation, is equal to the coefficient $(\tau\alpha)$ for direct radiation reaching the collector surface at an angle of 60°.

Correction factor for direct radiation R_b [29]:

$$R_b = \frac{cos\theta_\beta}{cos\theta_z} \quad (2)$$

Correction factor for diffused radiation R_d [29]:

$$R_d = \frac{1 + cos\beta}{2} \quad (3)$$

Correction factor for reflected radiation R_o [29]:

$$R_o = \frac{1 - cos\beta}{2} \quad (4)$$

The angle of incidence of solar radiation for any surface θ_β [29]:

$$\begin{aligned} cos\theta_\beta = {} & sin\delta\, sin\Phi\, cos\beta - sin\delta\, cos\Phi\, sin\beta\, cos\gamma + cos\delta\, cos\Phi\, cos\beta\, cos\omega \\ & + cos\delta\, sin\Phi\, sin\beta\, cos\gamma\, cos\omega + cos\delta\, sin\beta\, sin\gamma\, sin\omega \end{aligned} \quad (5)$$

where

Φ—latitude;
γ—receiver azimuth, deviation from the local meridian measured in relation to the south direction;
β—the inclination of the receiver relative to the horizon.

Solar zenith angle θ_z [29]:

$$cos\theta_z = cos\delta\ cos\Phi\ cos\omega + cos\delta\ sin\Phi \tag{6}$$

The solar declination δ is given by the formula [29]:

$$\delta = 23.45\ sin\left(360\frac{284+n}{365}\right) \tag{7}$$

where

n—next day of the year.

Hour angle ω [30]:

$$\omega = 15\left(\tau - 12^{00}\right) \tag{8}$$

where

τ—hour of the day.

Transmission-absorption coefficient for a given angle of incidence of solar radiation $(\tau\alpha)_{\theta\beta}$ [29]:

$$(\tau\alpha)_{\theta_\beta} = \frac{\tau_c\alpha_A}{1-(1-\alpha_A)\rho_d} \tag{9}$$

where

α_A—absorber absorption coefficient, and
ρ_d—radiation reflection coefficient from the phase boundary with different optical properties for diffusion radiation.

Total transmissivity of transparent coatings τ_c [29]:

$$\tau_c = \tau_r\tau_\alpha \tag{10}$$

Absorption of radiation τ_α by passing through a translucent material, according to the Bouguer law [29]:

$$\tau_\alpha = \exp\frac{-Kd}{cos\theta_2} \tag{11}$$

where

K—extinction coefficient, and
d—cover thickness.

The total transmissivity τ_r according to the Fresnel theory is given by the formula [29]:

$$\tau_r = \frac{1}{2}\left(\frac{1-r_\perp}{1+r_\perp} + \frac{1-r_\parallel}{1+r_\parallel}\right) \tag{12}$$

Reflectance coefficient for the parallel element $r_\parallel$ [29]:

$$r_\parallel = \frac{sin^2(\theta_2-\theta_1)}{sin^2(\theta_2+\theta_1)} \tag{13}$$

Reflectance coefficient for the perpendicular element $r_\perp$ [29]:

$$r_\perp = \frac{tg^2(\theta_2-\theta_1)}{tg^2(\theta_2+\theta_1)} \tag{14}$$

where

θ_1—angle of incidence.

Refraction angle θ_2 was determined according to Snell's law [29]:

$$n_1 sin\theta_1 = n_2 sin\theta_2 \quad (15)$$

where

n_1, n_2—refractive coefficients.

2.3.2. Calculations of Solar Chimney Parameters

Air temperature in the collector and air velocity were calculated by the method of successive approximations. The calculations were carried out in accordance with the Equations (16)–(23) and (26)–(35) used by Pluta in [28]. The calculations were made in the next steps:

(1) In the first approximation, the average air temperature in the collector t_f and air velocity in the collector cross-section v were assumed, while the collector glass temperature t_c was calculated from the formula:

$$t_c = 0.5\left(t_f + t_a\right) \quad (16)$$

where

t_f—average air temperature in the collector, and
t_a—ambient temperature.

(2) The absorber temperature t_A is determined from the equation:

$$t_A = t_f + 5^{\circ}\mathrm{C} \quad (17)$$

(3) For the assumed temperature t_f, the following parameters were read in the tables for dry air at 1013 kPa from [31]: thermal conductivity coefficient λ, Prandtl number Pr, kinematic viscosity coefficient ν and specific heat c_p.

(4) The formula for the Reynolds number Re is as follows:

$$Re = \frac{vD_h}{\nu} \quad (18)$$

where

v—air speed, and
D_h—characteristic dimension.

(5) For turbulent flow, the Nusselt number Nu is determined from the formula:

$$Nu = 0.036 Re^{0.8} Pr^{0.33} \left(\frac{D_h}{L}\right)^{0.055} \quad (19)$$

where

L—collector length.

(6) In the next step, the convective heat transfer coefficient h_{c1} is determined:

$$h_{c1} = \frac{Nu\lambda}{D_h} \quad (20)$$

(7) Then, the equivalent heat transfer coefficient from the radiation between the absorber and the glass h_{r1} is calculated as follows:

$$h_{r1} = \frac{\sigma\left(T_A^2 + T_c^2\right)(T_A + T_c)}{\left(\frac{1}{\varepsilon_A} + \frac{1}{\varepsilon_c} - 1\right)} \tag{21}$$

where

ε_A—absorber emissivity,
ε_c—glass emissivity, and
σ—Stefan–Boltzmann constant.

(8) The efficiency of the absorber F' is determined by the following formula:

$$F' = \frac{2h_{r1}h_{c1} + U_g h_{c1} + h_{c1}^2}{(U_g + h_{r1} + h_{c1})(U_d + h_{r1} + h_{c1}) - h_{r1}^2} \tag{22}$$

where

U_g—equivalent coefficient of heat loss through the front surface of the collector:

$$U_g = \frac{1}{\frac{1}{h_{c1}+h_{r1}} + \frac{1}{h_{c2}+h_{r2}}} \tag{23}$$

The coefficient of convective heat transfer from the glass surface to the environment caused by the wind h_{c2} was calculated from the formulas proposed by Jürges [32]:

for wind speed $v_w \leq 5$ m/s:

$$h_{c2} = 5.58 + 3.95v_w \tag{24}$$

for wind speed $v_w \geq 5$ m/s:

$$h_{c2} = 7.12v_w^{0.78} \tag{25}$$

h_{r2}—equivalent coefficient of heat transfer by radiation between the glass and the sky:

$$h_{r2} = \frac{\sigma\varepsilon_c\left(T_c^4 - T_{sky}^4\right)}{T_c - T_a} \tag{26}$$

T_{sky}—temperature of the sky.
U_d—heat loss coefficient of the collector bottom:

$$U_d = \frac{\lambda_i}{d_i} \tag{27}$$

λ_i—thermal conductivity coefficient of the collector's thermal insulation and
d_i—insulation thickness of the collector bottom.

(9) The formula for alternative loss factor U_L is as follows:

$$U_L = \frac{\left(U_d + U_g\right)\left[2h_{r1}h_{c1} + h_{c1}^2\right] + 2\,U_g U_d h_{c1}}{2h_{r1}h_{c1} + h_{c1}^2 + U_g h_{c1}} \tag{28}$$

(10) The mass flow of air $\dot{m}$ is determined by the following formula:

$$\dot{m} = vA_c\rho_{i,1} \tag{29}$$

where

A_c—collector cross-section and
$\rho_{i,1}$—air density at the inlet to the collector.

(11) The next step is to calculate the heat transfer coefficient F_R:

$$F_R = \frac{\dot{m}c_p}{A_A U_L}\left(1 - exp\frac{-A_A U_L F'}{\dot{m}c_p}\right) \tag{30}$$

where

A_A—absorber surface.

(12) The effective capacity of the collector $\dot{Q}$ is determined from the formula:

$$\dot{Q} = A_A F_R\left[G_\beta(\tau\alpha) - U_L(t_{i,1} - t_a)\right] \tag{31}$$

(13) Temperature of the air that leaves the collector channel $t_{i,2}$:

$$t_{i,2} = t_{i,1} + \frac{\dot{Q}}{\dot{m}c_p} \tag{32}$$

(14) The second approximation of the absorber temperature is obtained from the formula:

$$t_A = t_a + \frac{G_\beta(\tau\alpha) - \frac{\dot{Q}}{A_A}}{U_L} \tag{33}$$

(15) The second approximation of the average air temperature is obtained from the equation:

$$t_f = t_a + \frac{G_\beta(\tau\alpha) - \frac{\dot{Q}}{F' A_A}}{U_L} \tag{34}$$

(16) The second approximation of the collector glass temperature is calculated from the formula:

$$t_c = \frac{t_f h_{c1} + t_A h_{r1} + t_a U_g}{h_{c1} + h_{r1} + U_g} \tag{35}$$

(17) The second approximation of the air flow velocity is obtained from the equation from [33]:

$$v = \sqrt{\frac{2gH(T_i - T_a)}{T_i}} \tag{36}$$

where

H—height of the chimney,
g—gravitational acceleration, and
T_i—temperature at the inlet of the chimney.

For the glass temperature, collector absorber, average air temperature in the collector, and air velocity in the collector, the calculations are repeated from the beginning to obtain further approximations.

The electric power of the power plant was determined from the formula from [34]:

$$P_{el} = \Delta P_t \eta_t v A_{ch} \tag{37}$$

Pressure difference generated in the solar chimney [34]:

$$\Delta P_t = g\int_0^H (\rho_0 - \rho_i)\, dH \tag{38}$$

After simplification it was assumed [34]:

$$\Delta P_t = g(\rho_0 - \rho_i)H \tag{39}$$

where

η_t—efficiency of the turbine,
A_{ch}—the cross section of the chimney,
v—air speed,
ρ_i—air density at the inlet to the chimney, and
ρ_0—air density at the inlet to the collector.

3. Results

The solar chimney analysis was performed for a typical weather year. Climate data for Katowice provided by the Ministry of Investment and Development were used for the calculations [35]. The calculations were made for the changes in radiation intensity in each hour of the day. The analysis covered 8760 h throughout the year from 1 January to 31 December. In the calculations, the following quantities were used: total intensity of solar radiation on the horizontal surface, diffusive intensity of solar radiation on the horizontal surface, temperature of the dry bulb thermometer, wind speed, and temperature of the sky's radiation.

Figure 2 presents dimensions of the analyzed solar chimney.

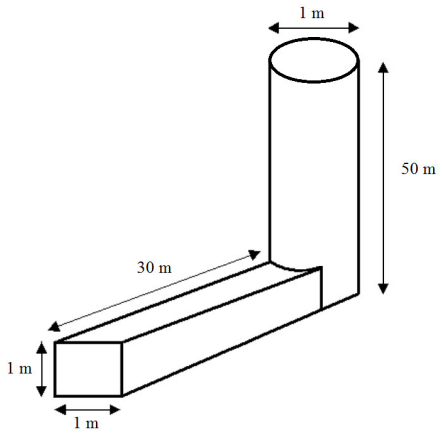

Figure 2. Dimensions of the analyzed solar chimney.

Table 1 presents the main assumptions for the calculations.

Table 1. The main assumptions for the calculations.

Parameter	Value
Gravitational acceleration	9.81 m/s^2
Stefan–Boltzmann constant	5.67×10^{-8}
Ground reflectivity	0.2
Absorber absorption coefficient	0.95
Coefficient of reflection of radiation from the interface	0.142
Extinction coefficient	-20 m^{-1}
Collector glass thickness	0.004 m
Absorber emissivity	0.95
Glass emissivity	0.95
Absorber area	30 m^2
Chimney height	50 m
Diameter of the chimney	1 m
Turbine efficiency	0.8

Figure 3a–d presents the average air temperature T_f in the collector in each quarter of the year. In the first and fourth quarters, the air temperature is the lowest, while the air temperature in the collector in the second and third quarters is the highest.

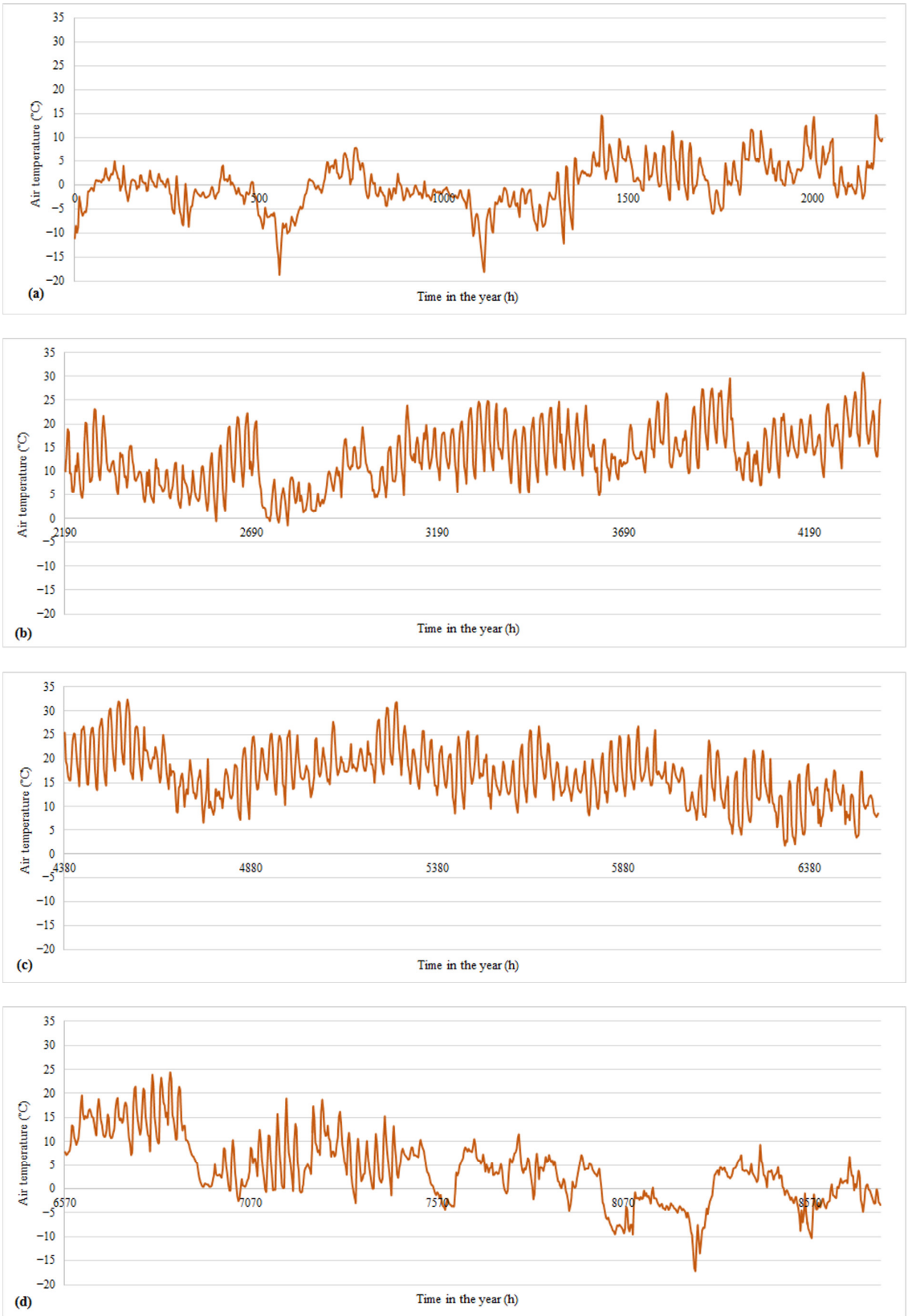

Figure 3. (**a**–**d**). Average air temperature in the collector in each quarter of the year.

Figure 4a–d shows the air temperature increase in the collector. The temperature increases for 4392 h per year. In the first quarter, the temperature increases for 898 h—the lowest is 0.01 K and the highest is 1.29 K, while the average increase is 0.45 K. In the second quarter, the temperature increases for 1389 h—the highest is 2.12 K, and the average is 0.79 K. In the third quarter, the temperature increases observed for 1298 h—the highest is 1.86 K and the average is 0.76 K. In the fourth quarter, the temperature increases for 807 h—the highest 1.35 K and the average is 0.42 K.

The lowest temperature increases are observed in the first and fourth quarters, and the smallest temperature increase, which amounts to 0.01 K, was on 29 March at 5.00 p.m. Low temperature increases result from low solar radiation heating the collector. The highest increases in air temperature occurred in the second quarter, which is related to higher solar radiation intensity. The maximum temperature increase occurred on 30 June at 10:00 a.m. and amounted to 2.12 K.

Figure 5a–d presents the air velocity in the solar chimney for each quarter of the year. The air speed depends on the air temperature increase in the collector, and therefore the highest air velocities are observed in the second and third quarters, when the air temperature increase in the collector is the highest. In the second quarter, the maximum achieved air speed was 3.70 m/s; in the third quarter, the maximum air speed was 3.47 m/s. In the first quarter, the maximum air speed of 3.00 m/s was achieved, while it was 2.97 m/s in the fourth quarter. The lowest air velocities, when the sun's rays fall on the installation, are similar to each other—in the second and third quarters, the air velocity is 0.3 m/s, 0.27 m/s in the first quarter, and 0.32 m/s in the fourth quarter.

The average air velocity in the first quarter is 1.68 m/s; when the air velocity is in the range of 2.00–3.00 m/s, it has a frequency of 29.65%; when the air velocity is in the range of 1.00–1.99 m/s, it has a frequency of 57.97%; when the air velocity is in the range of 0.28–0.99 m/s, it has a frequency of 12.38%. The average air velocity in the second quarter is 2.17 m/s; when the air velocity is in the range of 3.00–3.70 m/s, it has a frequency of 9.86%; when the air velocity is in the range of 2.00–2.99 m/s, it has a frequency of 48.31%; when the air velocity is in the range of 1.00–1.99 m/s, it has a frequency 36.21%; when the air velocity is in the range of 0.30–0.99 m/s, it has a frequency 5.62%. The average air velocity in the third quarter is 2.14 m/s; when the air velocity is in the range of 3.00–3.47 m/s, it has a frequency of 7.25%; when the air velocity is in the range of 2.00–2.99 m/s, it has a frequency of 51.46%; when the air velocity is in the range of 1.00–1.99 m/s, it has a frequency of 36.13%; when the air velocity is in the range 0.30–0.99 m/s, it has a frequency of 5.16%. The average air speed in the fourth quarter is 1.61 m/s; when the air velocity is in the range of 2.00–2.97 m/s, it has a frequency of 25.15% when the air velocity is in the range of 1.00–1.99 m/s, it has a frequency of 61.46%; when the air velocity is in the range of 0.32–0.99 m/s, it has a frequency of 13.38%.

Figure 6a–d shows the electric power generated by the solar chimney for each quarter of the year. The solar chimney system reached a maximum power of 5.51 W in the first quarter, 9.98 W in the second quarter, 7.97 W in the third quarter, and 4.95 W in the fourth quarter.

Figure 7 shows the amount of electricity generated during each month of the year. The installation can generate electricity at the greatest amount of 1366.84 Wh in May, and at the lowest amount of 204.86 Wh in December. In the winter months—November, December and January—the solar chimney produces the smallest amounts of electricity: 204.86–250.41 Wh. In May, June and July, the installation produces the greatest amounts of electricity, at 1202.05–1366.84 Wh.

Figure 4. (**a**–**d**). Temperature increase $\Delta T = T_f - T_a$ in the collector in each quarter of the year.

Figure 5. (**a**–**d**). Air speed in the solar chimney in each quarter of the year.

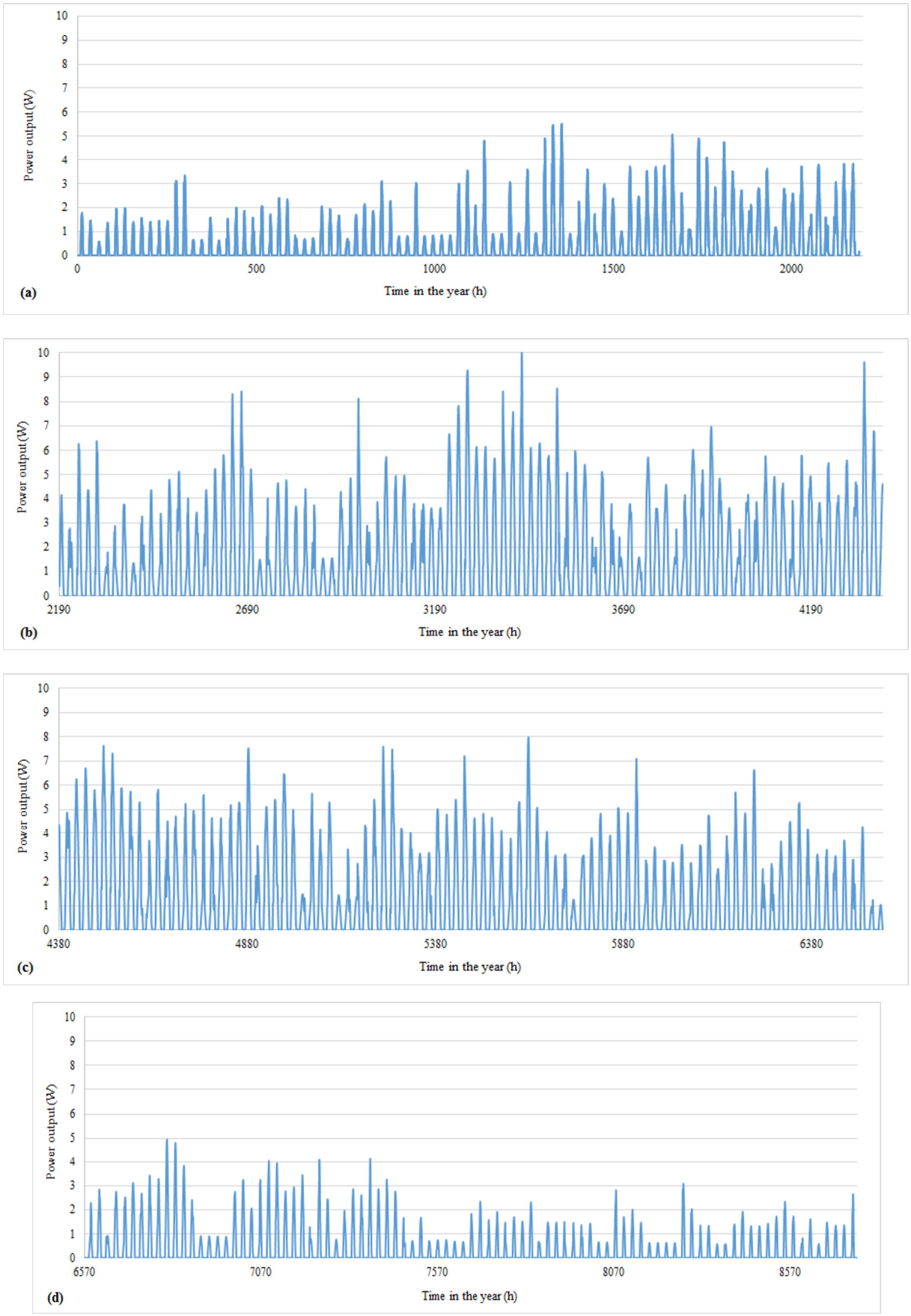

Figure 6. (**a**–**d**). Electric power generated by the solar chimney system for each quarter of the year.

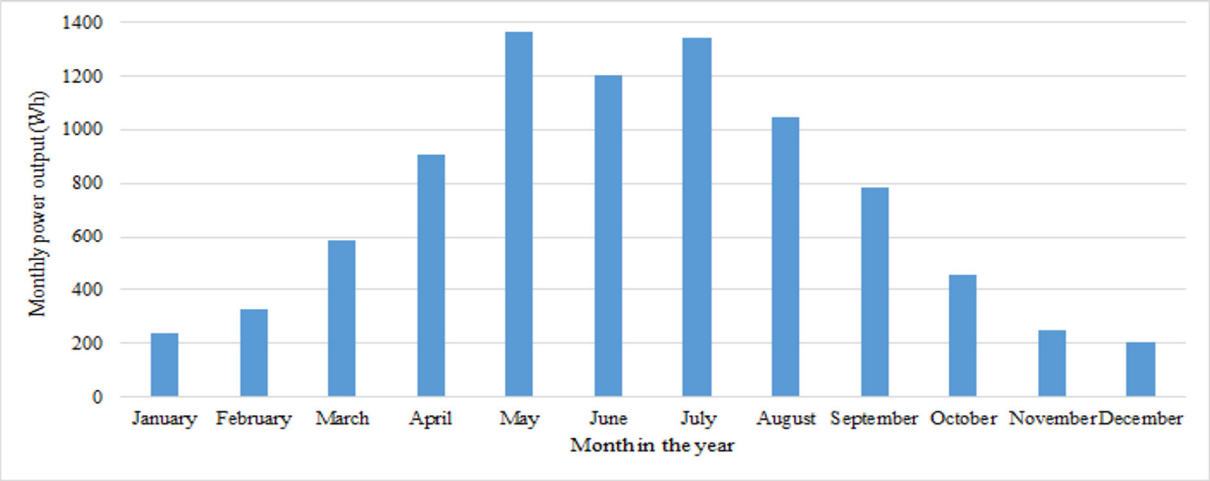

Figure 7. The amount of electricity produced in each month of the year.

Table 2 presents the amount of electricity which the solar chimney can produce in each quarter of the year. The solar chimney can generate the greatest amount of electricity in the second quarter, 3477.07 Wh, while the lowest amount of electricity is generated in the fourth quarter, 912.35 Wh. In the fourth quarter, the solar chimney generates 74% less electricity than in the second quarter. In the fourth quarter, the solar chimney generates 20% less electricity than in the first quarter and 71% less electricity than in the third quarter.

Table 2. The amount of electricity generated in each quarter of the year.

Quarter in the Year	Amount of Generated Electricity
I	1144.82 Wh
II	3477.07 Wh
III	3170.03 Wh
IV	912.35 Wh

4. Discussion

This article presents an analysis of the year-round operation of a solar chimney. In the literature, there are few works devoted to the year-round operation of the solar chimney, as the authors often present their results for one day of operation instead. The year-round analysis of the solar chimney system for the specific climate in Poland was desirable due to the variable intensity of radiation and cloud cover throughout the year in this country. In this work, a solar chimney with a rectangular collector situated on one side of the chimney was analyzed. In many publications, e.g., [3,4,6,7,12,19,20,22,23,25], the solar chimney was mainly analyzed with a circular collector located around the chimney, so there are not many studies using collectors of other shapes [24]. For a circular collector with an angle of 30°, the authors of [22] present the temperature of the absorber in this collector situated on the northern, southern, eastern and western side of the world. The absorber had a different temperature depending on location and the air did not warm up evenly in the collector. The use of a rectangular collector on one side of the chimney gives the possibility of increasing the temperature and thus higher air velocity by positioning the collector at an optimal angle and direction, thus obtaining the highest solar radiation for a given latitude.

A linear focusing collector can also be used in the proposed installation. The analyzed solar chimney can be used in the ventilation system of buildings where the air removed from the room can be heated using the entire surface of the collector. The presented solar chimney can also be used to recover waste heat—in this case, the heating medium could flow onto the lower side of the absorber, transferring heat along the whole length of the collector. In a solar chimney with a circular collector, the waste heat can be supplied to

the collector via a pipeline and can only heat some of the air flowing through the collector. Such a solution is presented in [36].

5. Conclusions

This article presents the main operating parameters of a solar chimney: average temperature of the air heated by the collector, air temperature increase, air speed and electric power achieved by the installation throughout the year. The most important conclusions of this study are:

(1) The highest air temperature increase, air velocity and generated electric power were achieved by the installation in the second and third quarters of the year, and the lowest in the fourth and first quarter.
(2) The greatest amount of electricity is generated in May, a little less in July, and the lowest in December. In May, the amount of energy generated is almost 7-fold greater than that in December.
(3) Due to the specific climatic conditions in Poland, in terms of the intensity of solar radiation and cloud cover, the maximum amount of electricity was generated in spring and summer.

Funding: This research received no external funding.

Institutional Review Board Statement: Not applicable.

Informed Consent Statement: Not applicable.

Data Availability Statement: Data for Energy Calculations of Buildings available online: https://www.gov.pl/web/archiwum-inwestycje-rozwoj/dane-do-obliczen-energetycznych-budynkow (accessed on 8 January 2022).

Conflicts of Interest: The author declares no conflict of interest.

References

1. Haaf, W. Solar Chimneys Part II: Premilinary test results from Manzanares Pilot Plant. *Int. J. Sol. Energy* **1984**, *2*, 141–161. [CrossRef]
2. Sivaran, P.M.; Harish, S.; Premalatha, M.; Arunagiri, A. Performance analysis of solar chimney using mathematical and experimental approaches. *Int. J. Energy Res.* **2018**, *42*, 2373–2385. [CrossRef]
3. Guo, P.; Li, J.; Wang, Y. Annual performance analysis of the solar chimney power plant in Sinkiang, China. *Energy Conv. Manag.* **2014**, *87*, 392–399. [CrossRef]
4. Larb, S.; Bouhdjar, A.; Chergui, T. Performance analysis of a solar chimney power plant in the southwestern region of Algeria. *Renew. Sustain. Energy Rev.* **2010**, *14*, 470–477. [CrossRef]
5. Bouabidi, A.; Ayadi, A.; Nasraoui, H.; Driss, Z.; Abid, M.S. Study of solar chimney in Tunisia: Effect of the chimney configurations on the local flow characteristics. *Energy Build.* **2018**, *169*, 27–38. [CrossRef]
6. Hu, S.; Leung, D.Y.C.; Chan, J.C.Y. Numerical modelling and comparison of the performance of diffuser-type solar chimneys for power generation. *Appl. Energy* **2017**, *204*, 948–957. [CrossRef]
7. Attig-Bahar, F.; Sahraoui, M.; Guellouz, M.S.; Kaddeche, S. Effect of the ground heat storage on solar chimney power plant performance in the South of Tunisia: Case of Tozeur. *Sol. Energy* **2019**, *193*, 545–555. [CrossRef]
8. Asnaghi, A.; Ladjevardi, S.M. Solar chimney power plant performance in Iran. *Renew. Sustain. Energy Rev.* **2012**, *16*, 3383–3390. [CrossRef]
9. Bernardes, M.A.; Voss, A.; Weinrebe, G. Thermal and technical analyses of solar chimneys. *Sol. Energy* **2003**, *75*, 511–524. [CrossRef]
10. Pretorius, J.P.; Kroger, D.G. Critical evaluation of solar chimney power plant performance. *Sol. Energy* **2006**, *80*, 535–544. [CrossRef]
11. Koonsrisuk, A.; Chitsomboon, T. Dynamic similarity in solar chimney modeling. *Sol. Energy* **2007**, *81*, 1439–1446. [CrossRef]
12. Asayesh, M.; Kasaeian, A.; Ataei, A. Optimization of a combined solar chimney for desalination and power generation. *Energy Conv. Manag.* **2017**, *150*, 72–80. [CrossRef]
13. Zuo, L.; Zheng, Y.; Li, Z.; Sha, Y. Solar chimneys integrated with sea water desalination. *Desalination* **2011**, *276*, 207–213. [CrossRef]
14. Ming, T.Z.; Gong, T.R.; de Richter, R.K.; Cai, C.J.; Sherif, S.A. Numerical analysis of seawater desalination based on a solar chimney power plant. *App. Energy* **2017**, *208*, 1258–1273. [CrossRef]
15. Niroomand, N.; Amidpour, M. New combination of solar chimney for power generation and seawater desalination. *Des. Water Treat.* **2013**, *51*, 7401–7411. [CrossRef]

16. Ferreira, A.G.; Maia, C.B.; Cortez, M.F.; Valle, R.M. Technical feasibility assessment of a solar chimney for food drying. *Sol. Energy* **2008**, *82*, 198–205. [CrossRef]
17. Eryener, D.; Kuscu, H. Hybrid transpired solar collector updraft tower. *Sol. Energy* **2018**, *159*, 561–571. [CrossRef]
18. Boutina, L.; Khelifa, A.; Touafek, K.; Lebbi, M.; Baissi, M.T. Improvement of PVT air-cooling by the integration of a chimney tower (CT/PVT). *Appl. Therm. Eng.* **2018**, *129*, 1181–1188. [CrossRef]
19. Jamali, S.; Nemati, A.; Mohammadkhani, F.; Yari, M. Thermal and economic assessment of a solar chimney cooled semitransparent photovoltaic (STPV) power plant in different climates. *Sol. Energy* **2019**, *185*, 480–493. [CrossRef]
20. Kiwan, S.; Al-Nimr, M.; Salim, I. A hybrid solar chimney/photovoltaic thermal system for direct electric power production and water distillation. *Sustain. Energy Tech. Assess.* **2020**, *38*, 100680. [CrossRef]
21. Liu, Q.; Cao, F.; Liu, Y.; Zhu, T.; Liu, D. Design and simulation of a solar chimney PV/T power plant in northwest China. *Int. J. Photoenergy* **2018**, *2018*, 1478695. [CrossRef]
22. Balijepalli, R.; Chandramohan, V.P.; Kirankumar, K. Development of a small scale plant for a solar chimney power plant (SCPP): A detailed fabrication procedure, experiments and performance parameters evaluation. *Renew. Energy* **2020**, *148*, 247–260. [CrossRef]
23. Sakir, T.; Piash, B.K.; Akhter, S. Design, Construction and Performance Test of a Small Solar Chimney Power Plant. *Glob. J. Res. Eng. Mech. Mech. Eng.* **2014**, *14*, 20–28.
24. Sreejaya, K.V.; Al-Kayiern, H.H.; Ul-Haq, S.I. Analytical analysis of roof top solar chimney for power generation. *Gilani J. Appl. Sci.* **2011**, *11*, 1741–1748. [CrossRef]
25. Silva, J.O.C.; Maia, C.B. Optimization of a small solar chimney. *Acta Polytech.* **2020**, *60*, 225–234. [CrossRef]
26. Area and Population in the Territorial Profile in 2021. Available online: https://stat.gov.pl/obszary-tematyczne/ludnosc/ludnosc/powierzchnia-i-ludnosc-w-przekroju-terytorialnym-w-2021-roku,7,18.html (accessed on 17 June 2022).
27. Wołoszyn, E. *Meteorologia i Klimatologia w Zarysie*; Wydawnictwo Politechniki Gdańskiej: Gdańsk, Poland, 2009.
28. Pluta, Z. *Podstawy Teoretyczne Fototermicznej Konwersji Energii Słonecznej*; Oficyna Wydaw, Politechniki Warszawskiej: Warszawa, Poland, 2006.
29. Duffie, J.A.; Beckman, W.A. *Solar Engineering of Thermal Processes*; John Wiley & Sons: Hoboken, NJ, USA, 1991.
30. Jastrzębska, G. *Ogniwa Słoneczne. Budowa, Technologia i Zastosowanie*; Wydawnictwo Komunikacji i Łączności: Warszawa, Poland, 2013.
31. Pudlik, W. *Wymiana i Wymienniki Ciepła*; Politechnika Gdańska: Gdańsk, Poland, 2012.
32. Jürges, W. The heat transfer at a flat wall. *Beih. Zum Gesundh. -Ingenieurwesen.* **1924**, *19*, 1227–1249.
33. Unger, J. *Konvektionsströmungen*; Teubner: Stuttgart, Germany, 1988.
34. Cao, F.; Zhao, L.; Guo, L. Simulation of a sloped solar chimney power plant in Lanzhou. *Energy Conv. Manag.* **2011**, *52*, 2360–2366. [CrossRef]
35. Data for Energy Calculations of Buildings. Available online: https://www.gov.pl/web/archiwum-inwestycje-rozwoj/dane-do-obliczen-energetycznych-budynkow (accessed on 8 January 2022).
36. Habibollahzade, A.; Houshfar, E.; Ahmadi, P.; Behzadi, A.; Gholamian, E. Exergoeconomic assessment and multi-objective optimization of a solar chimney integrated with waste-to-energy. *Sol. Energy* **2018**, *176*, 30–41. [CrossRef]